JOURNAL OF SOLID STATE CHEMISTRY **121,** 12–23 (1996)
ARTICLE NO. 0003

Mechanics of the Feldspar Framework; Crystal Structure of Li-Feldspar

Werner H. Baur[1] and Werner Joswig

Institut für Kristallographie und Mineralogie, Senckenberganlage 30, D-60054 Frankfurt am Main, Federal Republic of Germany

and

Gerd Müller

Fraunhofer-Institut für Silicatforschung, Neunerplatz 2, D-97082 Würzburg, Federal Republic of Germany

Received September 29, 1995; accepted October 9, 1995

DEDICATED TO THE MEMORY OF ALEXANDER F. WELLS

The crystal structure of $LiAlSi_3O_8$ was determined by single crystal X-ray diffraction, with 813 observed structure factors, refined to $R1 = 0.079$. Li-feldspar has the smallest unit cell volume of any feldspar with known crystal structure. Comparison of $LiAlSi_3O_8$ with various alkali feldspars, including the most open structure of $RbAlSi_3O_8$, illustrates the noncollapsible nature of the feldspar-type aluminosilicate framework. Noncollapsible frameworks in which the *T*–O–*T* angles (where *T* is a tetrahedrally coordinated atom; here Si and/or Al) antirotate when a tetrahedron rotates upon compression or expansion of the framework are mechanically stable and can maintain open pores without propping by inserted cations. The *T*–O–*T* angles serve as hinges between the rigid SiO_4 and AlO_4 tetrahedra. In monoclinic alkali feldspars, the antirotation of the *T*–O(A2)–*T* and *T*–O(C)–*T* angles balances the framework. Oxygen atom O(A2) is located on a mirror and connects the aluminosilicate double crankshafts of TO_4 tetrahedra into slabs parallel to (001), while atom O(C) is in a general position. In triclinic alkali feldspars, the pairs of angles around atoms O(Bo) and O(Bm), O(Co) and O(Cm), and finally O(Do) and O(Dm) (all in general positions) are in an equilibrium transmitted through oxygen atom O(A2). Despite its stability, the noncollapsible feldspar framework is extremely flexible. Individual *T*–O–*T* angles can vary in the feldspar framework by up to 27° without having a strong effect on the unit cell volume and without any significant effect on the overall mean *T*–O–*T* angle. The cell constant *a* relates to the short interatomic *M*–O(A2) distance (where *M* is an alkali atom) and the *T*–O(A2)–*T* angle. The unit cell volume (*V*) depends primarily on *a*, while *b* and *c* change little with variation of *V*. Thus the *T*–O(A2)–*T* angle is the linchpin of the framework mechanics. A further consequence of the noncollapsibility of the framework is that hydrogen feldspar does not collapse upon itself, even though it lacks an alkali atom.

INTRODUCTION

Some of the most open tetrahedral frameworks strongly resist collapse, even for radical change in the chemistry of embedded guests (ions or molecules). The empirically observed angular distortions in zeolite A and a computer simulation by Baur (1, 2) show that noncollapsibility is due to a self-regulating mechanism allowing framework distortion only within limits set by chemically possible values of the *T*–O–*T* angles (*T* means a tetrahedrally coordinated atom; here Si and/or Al) of the bridging oxygen atoms and which depends solely on the topological, symmetrical, and geometrical properties of the underlying three-dimensional (3D) nets. In contrast, the hinges of collapsible frameworks corotate cooperatively in the same sense. In noncollapsible frameworks the hinges antirotate, and compression at one hinge necessitates tension at another hinge. If the arrangement (the topology) of the flexible connections (the hinges, that is the oxygen atoms bridging the coordination tetrahedra) between the rigid parts is such that one hinge can only open up, while another closes, the framework cannot collapse, because the opening angle cannot open beyond being straight, and the closing angle must have a limit before its two sides interpenetrate. Or conversely, a framework can only be noncollapsible if parts of it must be stretched, while other parts are compressed, and vice versa. In this way an equilibrium between tension and compression can be reached.

[1] To whom correspondence should be addressed.

0022-4596/96 $12.00

In the context of a study of four-connected 3D nets Smith (3) found two basically different ways of linking plane 4.8^2 nets (plane nets where at each node two octagons and one tetragon meet) into 3D nets. In one case the resulting nets can easily contract and expand; Smith calls them flexible nets, and he identified seventeen simple ways of generating such flexible nets (the nets of the frameworks of phillipsite ($K_2Ca_2Al_5Si_{11}O_{32} \cdot 12H_2O$), merlinoite $K_5Ca_2Al_9Si_{23}O_{64} \cdot 24H_2O$), gismondine ($Ca_4Al_8Si_8O_{32} \cdot 18H_2O$), and paracelsian ($BaAl_2Si_2O_8$), belong here). On the other hand, there are 13 simple ways of obtaining inflexible nets, of which the feldspar net is one example. Inasmuch as Smith's (3) discussion does not refer to what happens to the hinges T–O–T in his flexible and inflexible nets it was originally only suspected by us, but was not certain, that they corresponded to what we would call collapsible and noncollapsible nets. One can check this suspicion by comparing expanded and compressed versions of such nets. One of the most expanded triclinic feldspar frameworks with known crystal structure is microcline ($KAlSi_3O_8$, (4)) and the most compressed feldspar framework known so far is that of high-pressure low albite determined at 3.78 GPa ($NaAlSi_3O_8$, (5)). The changes in the T–O–T angles between the expanded and the compressed version of the feldspar net are as expected for a noncollapsible net and as observed for zeolite A (1, 2, 6).

Müller (7) prepared by ion exchange in a melt of NaCl out of a sanidine, $KAlSi_3O_8$ (a potassium feldspar with Al/Si disorder), a sodium feldspar, $NaAlSi_3O_8$, and then turned this by acid treatment into a hydrogen feldspar, $HAlSi_3O_8$. Further exchange of the H-feldspar in a melt of $LiNO_3$ yielded Li-feldspar, $LiAlSi_3O_8$. The crystal structure of the H-feldspar was investigated by single crystal diffraction methods (8). The crystal structure of the Li-feldspar was modeled by distance least squares (DLS) methods (9) on the basis of experimentally determined unit cell constants (10).

We report here a single crystal structure determination of Li-feldspar and investigate the noncollapsible behavior of the feldspar framework.

EXPERIMENTAL

A powder of sanidine, $KAlSi_3O_8$, from Volkesfeld, Eifel, Germany (fraction from 60 to 250 μm) was twice treated for 3 days each at 1083 K in a melt of NaCl, then with concentrated sulfuric acid at 583 K, and finally with molten $LiNO_3$ at 563 K. From previous experiments (10) we know that the sample should be about 90% Li-exchanged and should contain only minor Na, K, Ca, and Ba.

Diffraction measurements on a single crystal were made at room temperature on an Enraf Nonius CAD4 diffractometer (Table 1). To cover the large mosaic spread of the crystallites ($\Delta\omega \sim 8°$) an ω-scan was used. The usual corrections were applied. All valid observations, including weak ones, were used in the refinement (see Kassner *et al.*, Ref. (11)). The unit cell parameters, refined on 15 reflections (Table 1), agree to 1.6 pooled estimated standard deviations with those reported for Li-exchanged sanidine from the same locality by Deubener *et al.* (10).

TABLE 1
Li-Feldspar, $LiAlSi_3O_8$, Crystal Data, Data Collection Parameters, and *R* Values

Chemical formula	$LiAlSi_3O_8$
Crystal system	Triclinic
Space group	$C\bar{1}$
a (Å)	7.862(6)
b (Å)	12.689(7)
c (Å)	7.056(4)
α (°)	95.95(5)
β (°)	116.73(5)
γ (°)	89.90(6)
V (Å^3)	624.5(16)
Z	4
Formula weight	984.76
D_x (Mg m^{-3})	2.618
Scan	ω
λ(Mo$K\alpha$) (Å)	0.7107
$(\sin\theta/\lambda)_{max}$ (Å^{-1})	0.59
μ(Mo$K\alpha$) (mm^{-1})	0.91
Size of crystal (μm × μm × μm)	150 × 150 × 60
Number of I_{hkl} measured	1728
Number of I_{hkl} accepted	1638
No. of unique F_{hkl} after averaging (NREF)	813
$R_{internal}$	0.021
h_{min}, h_{max}, k_{min}, k_{max}, l_{min}, l_{max}	−8, 8, −8, 8, −8, 8
Number of variables (NVAR)	117
$R1 = R(F) = \Sigma\,[\lvert F_0\rvert - \lvert F_c\rvert]/\Sigma\,\lvert F_0\rvert$	0.079
$wR2 = R(wF^2) = [\Sigma\, w(F_0^2 - F_c^2)^2/\Sigma\, w(F_0^2)^2]^{1/2}$	0.183
$GoF = [\Sigma\, w(F_0^2 - F_c^2)^2/(\text{NREF} - \text{NVAR})]^{1/2}$	1.20

The coordinates of the DLS refinement of Li-feldspar (10) were used as a starting model. The positions of the lithium atoms were located from difference Fourier maps. The largest correlation coefficient was 64% (between two temperature factors). Because the occupancy factors of Li(1) and Li(2) diverged they were fixed at one half of maximum occupancy. An attempt to position all lithium atoms within one fully occupied site worsened the $R1$ value to 0.082. The refinement was based on F^2. Table 2 gives atomic coordinates and displacement factors and Tables 3 and 4 give interatomic distances and bond angles.

RESULTS

The nomenclature for the Li-feldspar follows the conventions established by Megaw (16). In monoclinic (space

TABLE 2
Positional Coordinates, Displacement Parameters (U_{equ}, Å^2), and Populations (Pop.) of Atomic Sites for Li-Feldspar

Atom	x/a	y/b	z/c	U(equ)	Pop.
T(1o)	0.0088(4)	0.1534(3)	0.2079(5)	0.0248(12)	$\frac{1}{4}$Al, $\frac{3}{4}$Si
T(1m)	0.0028(4)	0.8155(4)	0.2314(5)	0.0240(13)	$\frac{1}{4}$Al, $\frac{3}{4}$Si
T(2o)	0.6791(4)	0.1018(3)	0.3051(5)	0.0244(11)	$\frac{1}{4}$Al, $\frac{3}{4}$Si
T(2m)	0.6685(4)	0.8757(3)	0.3571(5)	0.0242(11)	$\frac{1}{4}$Al, $\frac{3}{4}$Si
O(A1)	0.0075(13)	0.1288(8)	0.9739(13)	0.033(2)	1 O[a]
O(A2)	0.5649(11)	−0.0137(7)	0.2702(13)	0.030(2)	1 O
O(Bo)	0.8164(11)	0.0883(8)	0.1847(14)	0.038(3)	1 O
O(Bm)	0.8106(11)	0.8438(8)	0.2554(14)	0.040(3)	1 O
O(Co)	0.0032(11)	0.2803(8)	0.2813(13)	0.032(3)	1 O
O(Cm)	0.0166(11)	0.6845(8)	0.1974(12)	0.034(3)	1 O
O(Do)	0.2098(11)	0.1054(7)	0.3840(12)	0.027(2)	1 O
O(Dm)	0.1954(12)	0.8670(8)	0.4414(13)	0.035(2)	1 O
Li(1)	0.269(6)	−0.012(4)	0.163(7)	0.027(10)[b]	$\frac{1}{2}$Li
Li(2)	0.278(6)	0.032(4)	0.115(7)	0.027(10)[b]	$\frac{1}{2}$Li

[a] Refers to one oxygen atom.
[b] U_{iso} for lithium atoms.

group $C2/m$) feldspars M (the alkali ion) and oxygen atom O(A2) are located in fourfold special positions on a mirror and atom O(A1) is located on a diad axis. All other atoms are in general eightfold positions, named $T(1)$ and $T(2)$ for the tetrahedral cations and O(A), O(B), O(C), and O(D) for the oxygen atoms. In triclinic feldspars in space group $C\bar{1}$ all atoms are in fourfold general positions. Therefore, the atoms which in the monoclinic space group belonged to the same general set are split into two general positions each and distinguished by the suffixes m and o: thus, O(B) is split into O(Bo) and O(Bm) (see also Fig. 1 for the close relationship between the monoclinic and triclinic forms of the feldspar framework).

The crystal structure of $LiAlSi_3O_8$ is obviously an Si/Al-disordered feldspar: the overall mean T–O distance measures 1.642 Å as usual for a tetrahedral position occupied by 25% Al and 75% Si atoms. The Li site is split into two half-occupied sites 0.70(6) Å distant from each other. The distances Li(1)–O(A2) and Li(2)–O(A2) are the shortest of the distances around the Li atoms. Again this matches other feldspars. The distance from M to the oxygen atom A2 is always short (16) relative to the other oxygen atom neighbors (the cation M is located in the pores of the framework; it is either Li, Na, K or Rb). The a and c unit cell constants of $LiAlSi_3O_8$ are the shortest observed for any alkali feldspar under any physical conditions and the unit cell volume (V) is the smallest for any alkali feldspar of known crystal structure (Table 5). The T–O(A2)–T angle measures 124.9° and is the smallest observed for any T–O–T angle in an alkali feldspar, while the angle T–O(Bm)–T (162.0°) is the largest measured so far in any alkali feldspar (Table 6).

DISCUSSION OF THE CRYSTAL STRUCTURE OF $LiAlSi_3O_8$

Comparison with the DLS Structure

The samples of $LiAlSi_3O_8$ used by Deubener *et al.* (10) did not allow a precise determination of the crystal structure. But since the unit cell constants were measured with good accuracy from powder data the structure was modeled using the distance least squares (DLS) method of refinement. The average distance of the oxygen and T atoms from each other in the modeled and the actual crystal structure is 0.13 Å. The coordination tetrahedra were kept essentially rigid in the simulation. The agreement between the experimental structure and the simulated structure (10) can be judged best by the fit achieved for the T–O–T angles. On average, the eight crystallographically different T–O–T angles have been reproduced by the simulation within 6.6°. The differences between the angles around the pairs of A, B, and D atoms were correctly called. The differences between the two T–O–T angles around O(Co) and O(Cm) were inverted: T–O(Co)–T was calculated to be larger than T–O(Cm)–T, while the reverse is true. Since the difference between these two angles is smaller than for the other pairs of angles it

TABLE 3
***T*–O Bond Lengths, O–O Distances (Å), and O–*T*–O Angles (°) for $LiAlSi_3O_8$**

	T–O		O–*T*–O	O–O
T(1o)–O(A1)	1.644(8)	O(A1)–O(Co)	113.9(5)	2.757(12)
T(1o)–O(Co)	1.646(10)	O(A1)–O(Bo)	105.5(4)	2.628(9)
T(1o)–O(Bo)	1.659(6)	O(A1)–O(Do)	106.1(4)	2.651(11)
T(1o)–O(Do)	1.673(7)	O(Co)–O(Bo)	110.0(4)	2.706(12)
Mean	1.656	O(Co)–O(Do)	109.5(4)	2.711(11)
		O(Bo)–O(Do)	111.9(4)	2.760(8)
T(1m)–O(Bm)	1.630(5)	O(Bm)–O(Dm)	111.4(4)	2.704(8)
T(1m)–O(Dm)	1.643(8)	O(Bm)–O(A1)	107.5(4)	2.643(9)
T(1m)–O(A1)	1.647(9)	O(Bm)–O(Cm)	110.1(4)	2.700(11)
T(1m)–O(Cm)	1.665(10)	O(Dm)–O(A1)	106.7(4)	2.639(12)
Mean	1.646	O(Dm)–O(Cm)	109.6(4)	2.704(12)
		O(A1)–O(Cm)	111.5(4)	2.738(13)
T(2o)–O(Cm)	1.612(8)	O(Cm)–O(Dm)	112.7(4)	2.683(11)
T(2o)–O(Dm)	1.611(9)	O(Cm)–O(Bo)	111.0(4)	2.685(8)
T(2o)–O(Bo)	1.646(6)	O(Cm)–O(A2)	106.1(4)	2.612(12)
T(2o)–O(A2)	1.657(8)	O(Dm)–O(Bo)	110.9(4)	2.683(11)
Mean	1.632	O(Dm)–O(A2)	107.4(5)	2.633(11)
		O(Bo)–O(A2)	108.6(4)	2.682(8)
T(2m)–O(Bm)	1.608(6)	O(Bm)–O(Do)	109.0(4)	2.635(11)
T(2m)–O(Do)	1.627(8)	O(Bm)–O(Co)	108.7(4)	2.638(7)
T(2m)–O(Co)	1.639(8)	O(Bm)–O(A2)	110.0(4)	2.673(9)
T(2m)–O(A2)	1.654(8)	O(Do)–O(Co)	111.4(4)	2.698(11)
Mean	1.632	O(Do)–O(A2)	109.1(4)	2.672(11)
		O(Co)–O(A2)	108.7(4)	2.675(12)
Grand mean *T*–O distance	1.642			

TABLE 4

Comparison of the Environments of the Split-Atom Half-Occupied Li and Na Atom Positions in $LiAlSi_3O_8$ and $NaAlSi_3O_8$ (High Albite at 298 K (12)) with the Fully Occupied Na Position in High-Pressure Low Albite at 3.78 GPa (5) and the Mean Values for the First 4, 5, 6, and 7 Oxygen Atom Neighbors

	Li–O (Å)	Na–O (Å) 298 K	Na–O (Å) 3.78 GPa		Li–O (Å)	Na–O (Å) 298 K
M(1)–O(A2)	2.10(3)	2.364(2)	2.25(1)	*M*(2)–O(A2)	2.13(3)	2.352(2)
M(1)–O(Do)	2.24(4)	2.480(3)	2.33(2)	*M*(2)–O(Bo)	2.30(5)	2.522(3)
M(1)–O(Bo)	2.33(4)	2.561(4)	2.38(2)	*M*(2)–O(Do)	2.30(4)	2.568(3)
M(1)–O(A1)	2.38(4)	2.501(3)	2.45(1)	*M*(2)–O(A1)	2.32(3)	2.474(3)
M(1)–O(A1)	2.69(4)	2.815(3)	2.48(1)	*M*(2)–O(Cm)	2.53(4)	2.686(3)
M(1)–O(Dm)	2.86(4)	2.779(3)	2.96(1)	*M*(2)–O(A1)	2.84(4)	2.924(3)
M(1)–O(Co)	3.18(4)	3.125(3)	2.96(2)	*M*(2)–O(Bm)	3.00(5)	2.880(4)
Mean of 4	2.26	2.477	2.35	Mean of 4	2.26	2.479
Mean of 5	2.35	2.544	2.38	Mean of 5	2.32	2.520
Mean of 6	2.43	2.583	2.48	Mean of 6	2.40	2.558
Mean of 7	2.54	2.661	2.54	Mean of 7	2.48	2.629
Li(1)–Li(2)	0.70(6)					
Na(1)–Na(2)		0.704(4)				

seems that the modeled structure of the framework is fairly close to the actual framework of the Li-feldspar. The deviation in the *T*–O(C)–*T* angles is possibly connected with the assumption in the simulation that the Li atom is located only in one site, while in fact it is split into two positions each 0.5 Å distant from the modeled site of the Li atom.

Comparison with the Crystal Structure of High Albite at 298 K

The Li atom positions in $LiAlSi_3O_8$ are practically identical to the locations of the split Na atom sites in high albite as determined at 298 K (12). In both cases the two half atoms are 0.7 Å apart. The oxygen atom coordinations of both the Li and the Na atoms are highly irregular. The coordination of Na in albite (when described in split positions) is usually referred to as sevenfold. The geometry of the coordinations of Li in the Li-feldspar is best described as distorted tetrahedral inasmuch as the range from the shortest bond, Li–O(A2), to the longest bond, Li–O(A1), of the first four is smaller than the difference in length between the fourth and the fifth contact to either of the Li atoms. The energetic difference between the two half-sites must be extremely small: the same oxygen atoms coordinate the Li atoms in both cases, except that the O(A1) atom contacting Li(1) and Li(2) is crystallographically not identical but only equivalent in the two coordination spheres. The same argument is not true for the environment of the Na atoms in high albite. The question of the coordination of Na in the albites is complex, even though the amount of available information there is large (see the discussion in Ref. (12)). Whichever coordination is assumed for the Li atoms (or the Na atoms), the mean Li–O or Na–O distances are too long when compared with the sum of the Shannon ionic radii (17). However, as already pointed out by Shannon the radii apply only to fully occupied sites. The distances from cations in partly occupied sites to the surrounding anions are usually longer (17), as is found here too. The *T*–O–*T* angles to the three oxygen atoms with the shortest bonds to the Li atoms are on average smaller by 4.2° in $LiAlSi_3O_8$ than in high albite $NaAlSi_3O_8$ at 298 K (Tables 4 and 6). However, this is not related to the fact that the unit cell volume of Li-feldspar is 7% smaller than in high albite at 298 K (Table 5). Actually the *mean* *T*–O–*T* angle in the Li-feldspar is only 0.8° smaller than in the Na-feldspar (Table 6).

Comparison with the Crystal Structure of Low Albite at 3.78 GPa

The *V* and the mean *T*–O–*T* angles of the Li-feldspar are almost identical with those of the high pressure form of low albite, $NaAlSi_3O_8$, for which the crystal structure has been determined at a pressure of 3.78 GPa (5). In the high pressure form there is only *one* five-coordinated Na atom position. The Na–O bonds have been strongly compressed in such a way, relative to the low-pressure room temperature low albite form, that the mean distance Na–O is only slightly longer than the corresponding mean distance Li–O when we look at the closest 5, 6, or 7 oxygen atom neighbors of the alkali ions. Thus the *V* of the two forms of feldspar are similar. The differences in individual

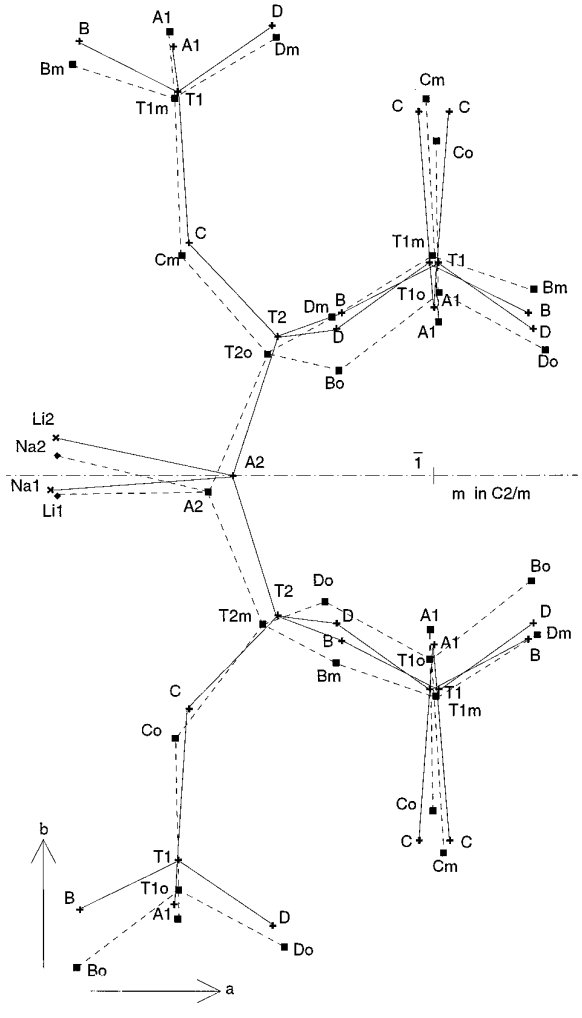

FIG. 1. Overlay of crystal structures of triclinic $LiAlSi_3O_8$ (broken lines) and monoclinic monalbite, $NaAlSi_3O_8$ (solid lines). In order to show the differences as well as possible the drawing is based on a metrically monoclinic unit cell with the cell constants averaged between those of the two compounds. The projection is approximately parallel [001].

T–O–T angles might be related to the different shape of the coordination polyhedra around the alkali atom in the two feldspars. It appears that replacing an Na atom by an Li atom within the feldspar framework is approximately equivalent to applying a pressure of 3.78 GPa to an albite, except that the pressure in $LiAlSi_3O_8$ is generated by internal pull (via the short Li–O bonds) instead of by external push.

NONCOLLAPSIBILITY AND FLEXIBILITY OF THE FELDSPAR FRAMEWORK

The crystal structure determinations of albite at high pressure and of Li-feldspar give us the details of the geometry of compressed feldspar frameworks, while the Rb-feldspar is an example of an expanded framework. This affords us the chance to follow the mechanics of the changes in that framework while it is breathing, as it were. The range of observed unit cell volumes of the alkali feldspars has been much expanded. The discussion is based on the data in Tables 5 and 6 (and Figs. 2 to 6) for several crystal structures of alkali feldspars. They are of monoclinic (space group $C2/m$) and triclinic ($C\bar{1}$) symmetry.

In Table 5 ten alkali feldspars are ordered by decreasing V. One might include many more entries into that table, however, the general principles can be illustrated by this selection. Table 6 lists seven of these feldspars with detailed values for their T–O–T angles and points out the regularities in their trends. The K-feldspars have been omitted from Table 6, because for microcline at 1278 K only the cell constants are known, with no crystal structure determination, while the inclusion of the room temperature data for orthoclase and microcline would have only cluttered the picture without changing its essence.

Changes in Individual T–O–T Angles with Volume

The most open alkali aluminosilicate feldspar is monoclinic $RbAlSi_3O_8$ (13) with a V of 736 Å^3. Its framework

TABLE 5
Unit Cell Constants a, b, and c (Å), α, β, and γ (°), Unit Cell Volumes V (Å^3), Framework Densities (FD) (as T/1000 Å^3), and References (Ref.) for Selected Alkali Feldspars

Feldspar	a	b	c	α	β	γ	V	FD	Ref.
$RbAlSi_3O_8$	8.820	12.992	7.161	90	116.24	90	736.0	21.7	(13)
$KAlSi_3O_8$, 1278 K microcline	8.728	12.994	7.224	90.68	115.66	87.81	735.1	21.8	(14)
$KAlSi_3O_8$, orthoclase	8.589	13.013	7.197	90	116.02	90	722.9	22.1	(15)
$KAlSi_3O_8$, microcline	8.572	12.964	7.223	90.65	115.95	87.64	721.2	22.2	(4)
$NaAlSi_3O_8$, 1060 K monalbite	8.297	12.994	7.144	90	116.01	90	692.2	23.1	(12)
$NaAlSi_3O_8$, 750 K high albite	8.234	12.955	7.143	92.00	116.17	90.06	683.3	23.4	(12)
$HAlSi_3O_8$	7.946	13.131	7.189	90	116.57	90	671.0	23.8	(8)
$NaAlSi_3O_8$, 298 K high albite	8.161	12.875	7.110	93.53	116.46	90.24	669.8	23.9	(12)
$NaAlSi_3O_8$, 3.78 GPa low albite	7.893	12.640	7.067	94.18	117.07	88.13	626.1	25.6	(5)
$LiAlSi_3O_8$	7.862	12.689	7.056	95.95	116.73	89.90	624.5	25.6	(this work)

Note. The space group is $C\bar{1}$ when triclinic cell constants are given and $C2/m$ when monoclinic cell constants are given.

TABLE 6
Comparison of Alkali Feldspar *T*–O–*T* Angles

Feldspar	Angles *T*–O–*T* around oxygen atoms (°)								Mean *T*–O–*T*
	O(A1)	O(A2)	O(Bo)	O(Bm)	O(Co)	O(Cm)	O(Co)	O(Dm)	
$RbAlSi_3O_8$	144.9	143.8	152.2		130.9		142.1		142.4
$NaAlSi_3O_8$, 1060 K monalbite	145.4	134.2	151.1		134.5		141.2		141.7
$NaAlSi_3O_8$, 750 K high albite	144.3	131.2	146.6	155.8	132.4	134.0	138.2	145.6	141.0
			+4.5	−4.7	+2.1	+0.5	+3.0	−4.4	
			151.2		133.2		141.9		
[$HAlSi_3O_8$	152.3	134.8	153.9		132.9		145.8		144.0]
$NaAlSi_3O_8$, 298 K high albite	143.2	129.7	141.4	158.8	130.4	134.6	135.3	149.5	140.4
			+9.7	−7.7	+4.1	−0.1	+5.9	−8.3	
			150.1		132.5		142.4		
$NaAlSi_3O_8$, 3.78 GPa low albite	139.5	130.1	135.4	159.4	125.3	137.4	135.5	153.8	139.6
			+15.7	−8.3	+9.2	−2.9	+5.7	−12.6	
			147.4		131.4		144.7		
$LiAlSi_3O_8$	143.6	124.9	135.0	162.0	129.7	135.2	133.9	152.5	139.6
			+16.1	−10.9	+4.8	−0.7	+7.3	−11.3	
			148.5		132.5		143.2		
Maximal difference between mean *T*–O–*T*	5.9	18.9	4.8		3.6		3.5		2.8
Maximal difference between individual *T*–O–*T* angles	5.9	18.9	17.2	10.9	9.2	6.5	8.2	12.6	

Note. The noncollapsible framework of feldspar with antirotation of the *T*–O–*T* angles. Comparison of expanded monoclinic and triclinic feldspar frameworks with compressed triclinic frameworks: *T*–O–*T* angles (°), the means for the triclinic cases for O(B), O(C), and O(D), the deviations from the values for monalbite, the overall means of the *T*–O–*T* angles, and the maximal differences between each type of angle, both after averaging the angles at O(B), O(C), and O(D) and individually. For further details see text, for references see Table 5. The entries for $HAlSi_3O_8$ are not used in the means and the differences listed below.

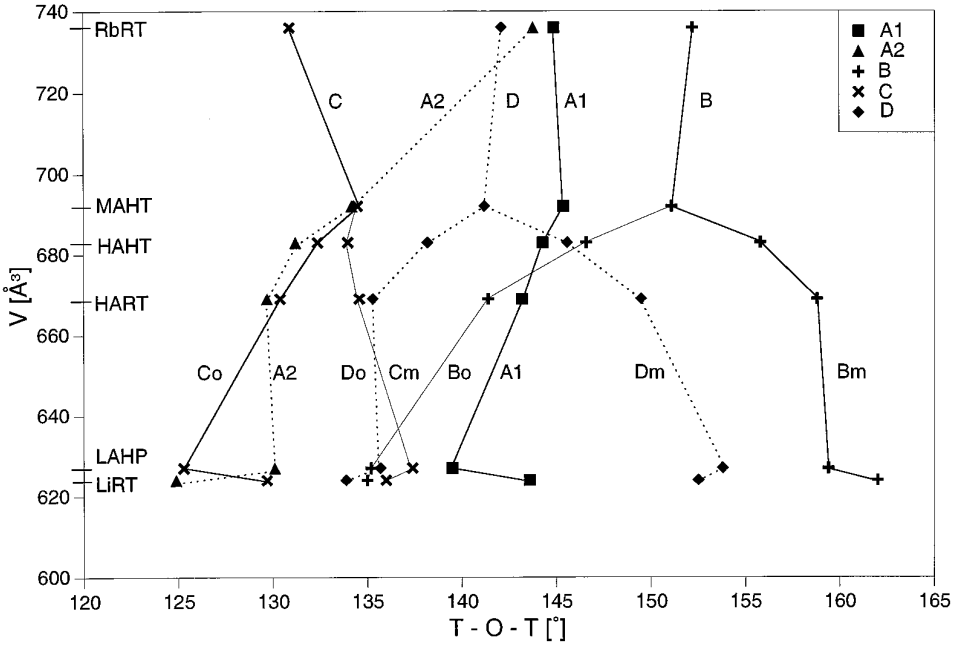

FIG. 2. Unit cell volume [Å^3] as a function of *T*–O–*T* angles (°) in six alkali feldspars. The meaning of the notations are: RbRT, Rb-feldspar at room temperature; MAHT, monalbite, $NaAlSi_3O_8$, monoclinic albite at 1060 K; HAHT, high albite at 750 K; HART, high albite at room temperature; LAHP, low albite at 3.78 GPa; LiRT, Li-feldspar at room temperature. For further information and references see Table 5 and text. The entered points are connected arbitrarily by solid or broken lines in order to guide the eye.

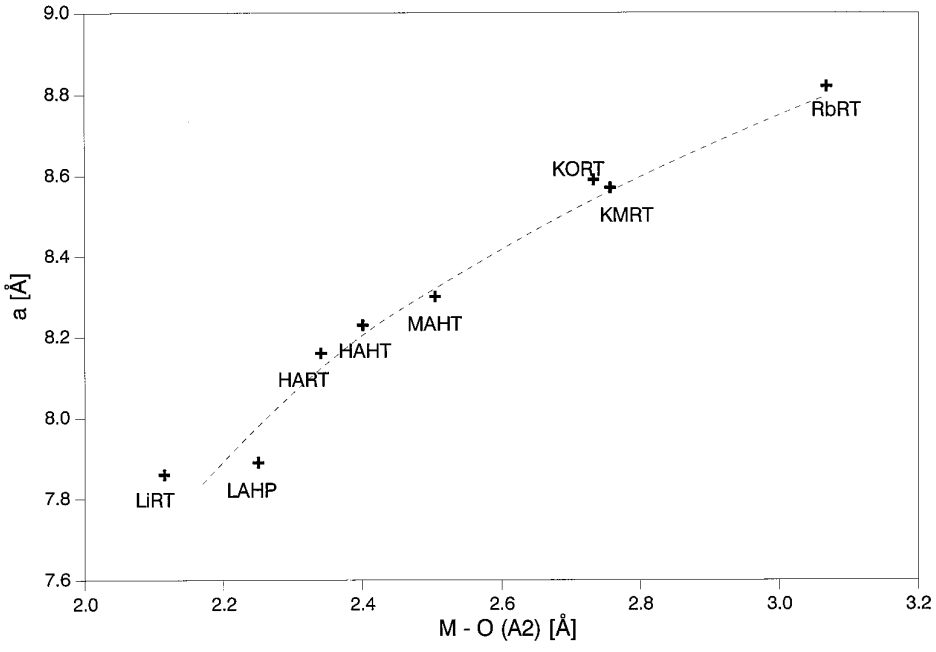

FIG. 3. Plot of unit cell constant a (Å) vs distance M–O(A2) (Å) for eight alkali feldspars. KORT stands for monoclinic orthoclase, $KAlSi_3O_8$, at room temperature; KMRT for triclinic microcline, $KAlSi_3O_8$, at room temperature. For other symbols see legend to Fig. 2. The curve through the data points is (as in the following figures) meant to guide the eye and is not based on a fit.

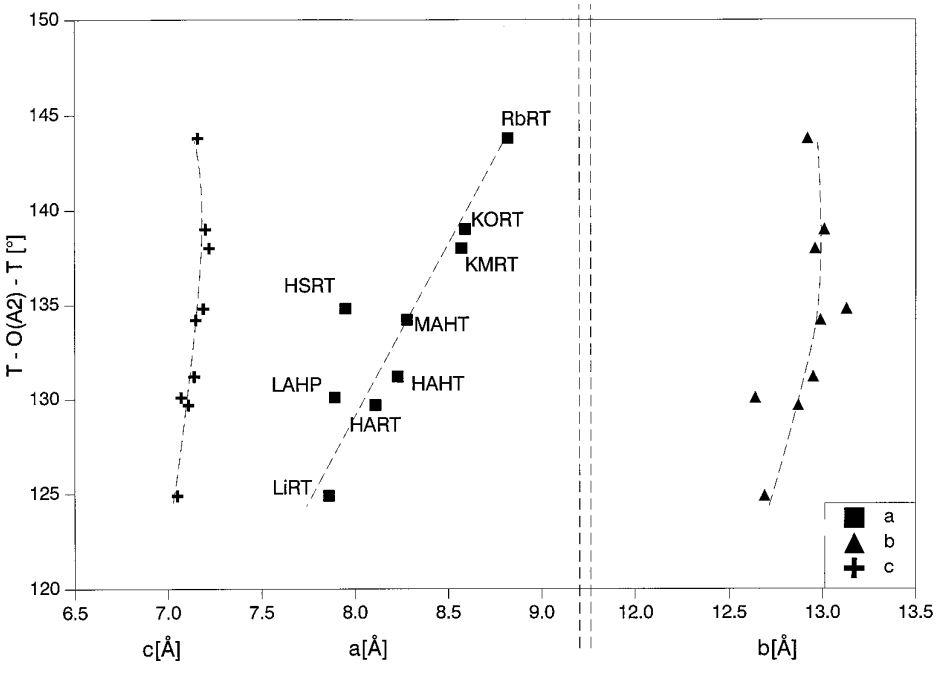

FIG. 4. Plots of unit cell constants a, b, and c (Å) vs T–O(A2)–T angle (°) for eight alkali feldspars and H-feldspar. For notations see legends to Figs. 2 and 3.

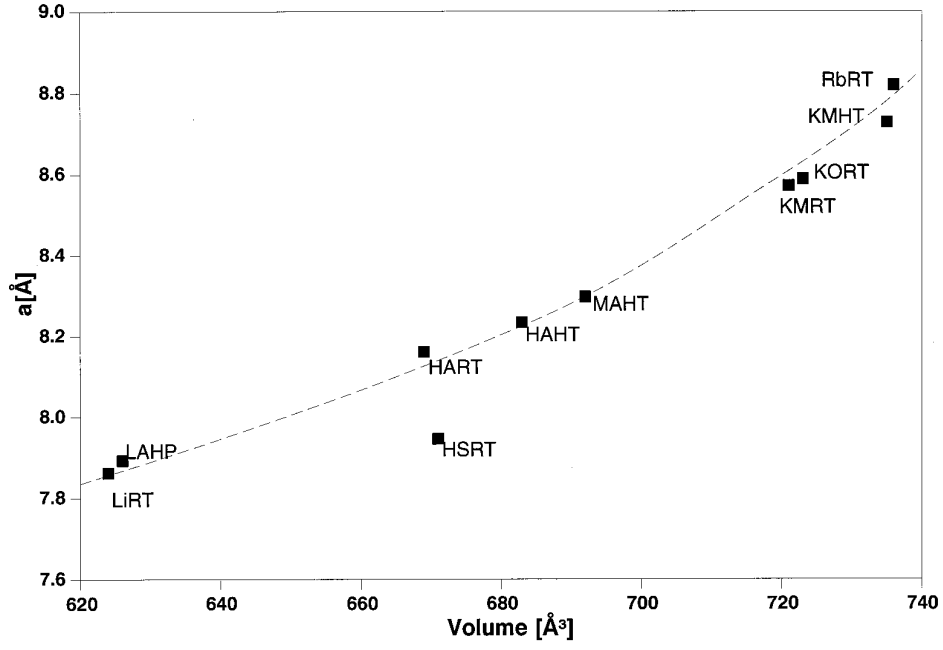

FIG. 5. Plot of unit cell constant a (Å) vs unit cell volume (Å^3). KMHT stands for triclinic microcline, $KAlSi_3O_8$, at 1278 K. For other notations see legends to Figs. 2 and 3.

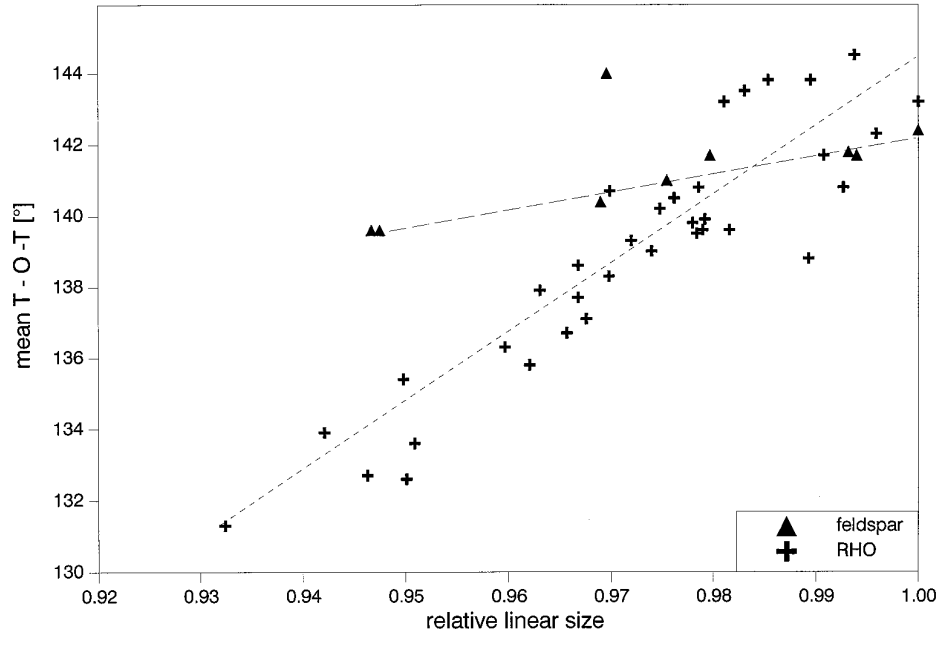

FIG. 6. Plot of mean T–O–T (°) angle vs relative linear size of the frameworks of zeolite RHO (in space group $I\bar{4}3m$, 35 points (23)) and of feldspar (same nine entries used as in Fig. 4). The linear size taken for RHO is the ratio of each entered unit cell constant over the largest observed cell constant (14.9771 Å); for feldspar it is the ratio between the cube root of the individual unit cell volumes over the cube root of the cell volume of the Rb-feldspar. The outlier among the feldspars is $HAlSi_3O_8$. See also text.

density (FD) is 21.7 T atoms per 1000 Å^3 (Table 5) and approaches the density of the densest zeolites. It has a volume 17.9% larger than the most compact feldspar, $LiAlSi_3O_8$, but in linear terms this amounts to only 5.6% (cube root). The reduction in V from Rb-feldspar to monalbite (monoclinic high temperature, 1060 K) high albite, $NaAlSi_3O_8$, is 6.3% (linearly 2.1%). The mean T–O–T angle in monalbite is only 0.7° smaller than in the Rb-feldspar. The individual T–O–T angles around oxygen atoms O(A1), O(B), and O(C) change little. Those around O(A2) and O(C) change in an opposite sense (they antirotate): the T–O(A2)–T angle decreases by 9.6°, while the T–O(C)–T angle increases by 3.6° (atom O(A2) is located in special equivalent position 4*i*, thus it occurs only half as often as atom O(C) which is sited in general position 8*j*). In a collapsible framework, such as the frameworks of quartz or tridymite, SiO_2, or of natrolite, $Na_2Al_2Si_3O_{10} \cdot 2H_2O$, all T–O–T angles corotate, they change cooperatively, upon a change in volume.

At lower temperature and after a reduction in unit cell volume (from 692.2 to 683.3 Å^3 at 750 K) high albite, $NaAlSi_3O_8$, becomes triclinic (space group $C\bar{1}$); atoms O(A1), located on a twofold axis, and O(A2), on a mirror plane in space group $C2/m$, turn into general positions. Oxygen atom positions O(B), O(C), and O(D) are split each into two general positions. The T–O–T angles at the split positions diverge, the angles named o assume smaller values and the angles named m increase, and their averages stay remarkably constant throughout the reduction in V down to the compressed forms (Fig. 2). Thus the three pairs of T–O–T angles effectively antirotate through the medium of oxygen atom O(A2). As atom O(A2) moves to smaller angles T–O(A2)–T, atom O(Bo) must move to smaller angles T–O(Bo)–T and angle T–O(Bm)–T must open up. Since the T–O(A1)–T angle does not move drastically over the whole range of unit cell volumes, only the T–O(A2)–T angle changes appreciably; it is reduced by 18.9° from $RbAlSi_3O_8$ to $LiAlSi_3O_8$ (which in a general way was already commented upon by Smith and Brown (19) on the basis of limited data). So while in monoclinic feldspars it is the movement of O(A2) vs O(C), in the triclinic feldspars it is O(A2) vs the three pairs of B, C, and D oxygen atoms. This is demonstrated by the different movements of the angles in the two most dense modifications of the feldspars, the high pressure form and the Li form. The T–O(A2)–T angle in $LiAlSi_3O_8$ is reduced in response to the short Li–O(A2) distance, while the angles T–O(Co)–T and T–O(Cm)–T, as well as the angles T–O(Bo)–T and T–O(Bm)–T, make pair-wise coupled movements relative to the high pressure form of albite (5) (Figs. 1 and 2). In this case atoms O(Do) and O(Dm) hardly participate in the rearrangement. Thus, overall the means of the angles around O(Bo) and O(Bm), O(Co) and O(Cm), and O(Do) and O(Dm) change little throughout this series of frameworks.

However, when we look at the individual T–O–T angles and their differences throughout the expanded and the compressed feldspar frameworks, the mean absolute deviation of their extreme values is 11.2° (that is the average of the entries in the last line of Table 6). The single largest difference in one feldspar is 27° between the topologically equivalent angles around O(Bo) and O(Bm) in the Li-feldspar. The single largest individual difference of the same angle between two compounds is around atom O(A2) between the Li- and the Rb-feldspar. Therefore, it shows again, as it did for zeolite A (1, 2), that the noncollapsible frameworks are remarkably flexible even when compared with the collapsible frameworks.

Minor Changes in Mean T–O–T Angle with Volume

Nevertheless the overall mean T–O–T angle changes only by 2.8° between the most open and the most compressed feldspar. Its contribution to the linear size reduction between the Rb- and the Li-feldspars can be estimated by obtaining the percentage deviation between the sines of the mean angle (T–O–T)/2 of the two crystal structures. This is a measure of how much closer the T atoms are, on average, to each other in the Li than in the Rb form (this is true as long as the mean distance T–O remains constant between the structures). The result is 0.9% and this amounts to only about one sixth of the 5.6% linear reduction in overall size of the unit cell. No other tetrahedral aluminosilicate framework is known to us where the decrease in T–O–T angles contributes so little to the volume reduction. Obviously the crumpling of the noncollapsible feldspar framework happens on a larger scale within the rings of coordination tetrahedra and cannot be measured by the changes in the overall mean T–O–T angle alone.

The trends discussed above are not influenced by Si/Al order within the tetrahedral coordinations in the framework. If the values for high albite at 298 K in Tables 5 and 6 were replaced by the corresponding values for a refinement of a low albite at room temperature with ordered Si and Al sites, the picture developed here would not change.

Trends in the Geometry of the Feldspar Framework

Relations and trends between various geometrical data of feldspars have been much discussed. Thus Fig. 2 looks similar to Fig. 6 from Brown *et al.* (18) where angles T–O–T were plotted against the trend of a plot of unit cell constants b and c in feldspars. It seems simpler, however, to plot directly against the volume as is done here, inasmuch as we are discussing the changes with vol-

ume among the feldspars. We mention here Megaw's observation (20) that the angle T–O(A2)–T increases markedly with the size of the M cation and Smith's and Brown's (21) finding that the a cell constant increases with cation size. Since we can now follow these trends down to smaller unit cell volumes we see that for the alkali feldspars the cell constant a depends approximately linearly on the shortest distance M–O(A2) (Fig. 3). Furthermore, a is approximately a function of the angle T–O(A2)–T (Fig. 4), while cell constants b and c are largely independent of that angle. At larger T–O(A2)–T angles b and c seem to decline in their values. Related to this is the observation that upon heating microcline, $KAlSi_3O_8$, from room temperature to 1278 K only a increases with temperature, while b and c remain relatively constant and decline at higher temperatures (especially b (14)). Openshaw *et al.* (14) commented on this in terms of an inherent difference between K- and Na-feldspar (the latter shows thermal expansion of its b and c constants as well). The main difference, however, is that sodium feldspar is in the medium range of possible unit cell volumes for the aluminosilicate feldspar frameworks, while thermally expanded K-feldspar pushes at the end of the range close to the volume of the Rb-feldspar (Table 5).

Atom O(A2) and the T–O(A2)–T Angle Play a Pivotal Role in the Feldspar Structure

Thus, the unit cell volume for the alkali feldspars is mostly a function of cell constant a (Fig. 5). Therefore, the T–O(A2)–T angle emerges as the linchpin of the mechanics of this framework. This is not surprising since oxygen atom O(A2) connects the aluminosilicate double crankshafts of TO_4 tetrahedra into slabs parallel to the plane (001) (which are a major feature of the architecture of the feldspar framework (16)) and interacts strongly with the M cations in the pores of the framework (19).

This is also shown in Fig. 1 in terms of its role in the antirotating behavior of the o and m atoms of the triclinic feldspar. The short Li–O(A2) distance pulls atom O(A2) away from the two $T2$ tetrahedra (see the left of Fig. 1), therefore, the angle T(2o)–O(A2)–T(2m) is smaller than in monalbite. The heights of atoms T(2o) and T(2m) in the c direction change oppositely and both coordination tetrahedra rotate slightly around an axis through the T atoms and the midpoint of their O(B)–O(D) edge. The T–O–T angles around the o and m oxygen atoms change their values in an antirotating sense at the O(B) and O(D) oxygen atoms (see Table 6 for the actual values of the involved T–O–T angles). The compensating changes in the T–O–T angles in $LiAlSi_3O_8$ as compared to monalbite are clearly discernible in Fig. 1.

The recognition of the framework of feldspar as a third example of a self-regulating noncollapsible framework similar in this respect to the frameworks of faujasite and zeolite A (1, 2) may explain why no pure Cs-feldspar is known. The limit of expansion apparently is reached with Rb-feldspar (V = 736 Å^3). At the same unit cell volume the thermal expansion of microcline levels off (14). Smith and Brown (21) conclude that the change of trends observed by them on substituting Rb for K "is more difficult to explain and must be due to some sort of expansion limit in the framework." Their observation fits well with our findings.

Hydrogen Feldspar

The hydrogen feldspar (8) is an example of a feldspar framework with essentially empty pores and without an M atom. This is so because the hydrogen atom seems to be delocalized over the various oxygen atom positions. Even if it were localized it certainly would not have a high coordination number. It is the closest we have so far to a feldspar framework left to its own devices without the influence of bonds from an M atom to the oxygen atoms. An even better comparison could be made with a feldspar-type SiO_2 modification, but so far this is unknown. The most affected T–O–T angle in the H-feldspar, judged by the differences to the angles in the Na-feldspars of similar volume, is around O(A1); the next largest difference involves atom O(A2). This validates Megaw's (20) tetrahedral tilt model which is based mostly on the coordination triangle of two O(A1) oxygen atoms and one O(A2) atom around the M atom. In any event, the poor fit of $HAlSi_3O_8$ in the plots of Figs. 4 and 5 shows clearly that it does not belong to the population of alkali feldspars. Despite the fact that the volume requirements of hydrogen atoms are minimal, the feldspar framework does not collapse. Its unit cell volume is a trifle larger than for an Na-feldspar. Thus, the empty-pored feldspar-type $HAlSi_3O_8$ behaves essentially as the noncollapsible open frameworks of zeolite A and of faujasite even though it has a much denser framework than these zeolites.

Comparison of Linear Size and T–O–T Angle in Feldspar and Zeolite RHO

It is counterintuitive to assume that in an expanded framework a T–O–T angle would be small (as T–O(C)–T is in $RbAlSi_3O_8$) or that in compressed frameworks T–O–T angles would be open (as T–O(Bm)–T, T–O(Cm)–T, and T–O(Dm)–T are in high-pressure low albite and in $LiAlSi_3O_8$ when compared with the expanded structures). However, that is what happens in frameworks where T–O–T angles antirotate when tetrahedra rotate around themselves or around a linchpin (such as atom O(A2) in feldspars) upon a change in V. The intuitive assumption is only correct for collapsible frameworks (e.g., natrolite, $Na_2Al_2Si_3O_{10} \cdot 2H_2O$ (6, 22), or RHO-type zeolites, e.g.,

$Na_9Cs_3Al_{12}Si_{36}O_{96} \cdot 5H_2O$ (23, 24)) where the mean and the individual T–O–T angles change substantially and linearly with the cube root of the unit cell volume. In Fig. 6 the relationship between mean T–O–T angle and the relative linear size of the framework is shown for a collapsible framework (RHO-type structure in space group $I\bar{4}3m$), and for the noncollapsible feldspar. Obviously the slope is much steeper for zeolite RHO than for feldspar. Such is the noise in the plot that the different slope for feldspar would not be clearly noticeable without the points for the high-pressure low albite and for $LiAlSi_3O_8$ (the two leftmost points). The outlier among the feldspar points is $HAlSi_3O_8$. Almost 2/3 of the linear size reduction in zeolite RHO-type materials is attributable to the reduction in T–O–T angles (compared to 1/6 in feldspar, see above).

CONCLUSION

Noncollapsible frameworks are in a mechanical equilibrium and can maintain open pores without needing to be propped by inserted cations or molecules. The feldspar framework is of this noncollapsible type. In the monoclinic varieties of the alkali feldspars it is the antirotation of the T–O(A2)–T and T–O(C)–T angles which balances the framework. In the triclinic alkali feldspars it is the pairs of angles around atoms O(Bo) and O(Bm), O(Co) and O(Cm), and O(Do) and O(Dm) which are in antirotating equilibrium via atom O(A2). These pairs of oxygen atoms are symmetrically equivalent in the monoclinic feldspars.

A further consequence of the noncollapsibility of the framework is that hydrogen feldspar does not collapse upon itself, even though it lacks an alkali atom.

Despite its mechanical stability the noncollapsible feldspar framework is extremely flexible:

1. Individual T–O–T angles vary in the alkali feldspar framework among differently cation-exchanged feldspars by up to 19° without having a dramatic influence on the overall dimensions of the framework (that is on the unit cell volume) and without changing the overall mean T–O–T angle to any great degree.
2. Topologically equivalent T–O–T angles within one feldspar (the triclinic Li-feldspar) can differ by 27°.

This is similar to the observation made on zeolite A (1, 2). Noncollapsible frameworks need not be and are not rigid. Actually, they achieve their noncollapsibility and their stability by being extremely flexible within certain limits. In this they differ from most man-made structures on the surface of Earth, which additionally depend for their stability on a compressive outside force (gravity). Noncollapsible 3D structures share their kind of stability with the many aesthetically pleasing graceful examples of noncollapsible frameworks (however, not three-dimensionally periodic) invented and built as sculptures by Kenneth Snelson (25). These are also based on the interplay of compression elements (in his case provided by steel pipes) and tension elements (wire ropes). Both types of frameworks might be models for stable structures to be built in gravity-free environments outside of Earth.

PROGRAMS

The computer programs used in this work were SHELXL-93 (26) and SADIAN90 (27).

ACKNOWLEDGMENTS

What we call a framework in our context is a physical representation of a three-dimensional net of primary bonds. This way of looking at certain crystal structures and investigating their topological and geometrical properties was introduced by A. F. Wells in an early paper (28) and developed by him over the years (29–31). The subject of three-dimensional four-connected nets, of which the feldspar framework is an example, was first explored by him in 1954 (32). His pioneering work is gratefully acknowledged. We thank R. X. Fischer, J. V. Smith, and T. A. Vanderah for critical comments on an earlier version of this paper and D. Büdel for drafting and help with word processing.

REFERENCES

1. W. H. Baur, *J. Solid State Chem.* **97,** 243 (1992).
2. W. H. Baur, *Proc. Polish-German Zeolite Symp. Toruń* 11 (1992).
3. J. V. Smith, *Mineral. Mag.* **36,** 640 (1968).
4. A. Blasi, A. Brajkovic, C. De Pol Blasi, E. E. Foord, R. F. Martin, and P. F. Zanazzi, *Bull. Mineral.* **107,** 411 (1984).
5. R. T. Downs, R. M. Hazen, and L. W. Finger, *Am. Mineral.* **79,** 1042 (1994).
6. W. H. Baur, *Proc. 2nd Polish-German Zeolite Symp. Toruń* in press (1995).
7. G. Müller, *Nature* **332,** 435 (1988).
8. H. Paulus and G. Müller, *Neues Jahrb. Mineral. Monatsh.* 481 (1988).
9. C. Baerlocher, A. Hepp, and W. M. Meier, "DLS-76, A Program For the Simulation of Crystal Structures by Geometric Refinement." ETH, Zürich, 1978.
10. J. Deubener, M. Sternitzke, and G. Müller, *Am. Mineral.* **76,** 1620 (1991).
11. D. Kassner, W. H. Baur, W. Joswig, K. Eichhorn, M. Wendschuh-Josties, and V. Kupčik, *Acta Crystallogr. Sect. B* **49,** 646 (1993).
12. J. K. Winter, F. P. Okamura, and S. Ghose, *Am. Mineral.* **64,** 409 (1979).
13. M. Gasperin, *Acta Crystallogr. Sect. B* **27,** 854 (1971).
14. R. E. Openshaw, C. M. B. Henderson, and W. L. Brown, *Phys. Chem. Mineral.* **5,** 95 (1979).
15. A. Dal Negro, R. De Pieri, and S. Quareni, *Acta Crystallogr. Sect. B* **34,** 2699 (1978).
16. H. D. Megaw, "The Feldspars" (W. S. MacKenzie and J. Zussmann, Eds.), p. 2. University Press, Manchester, 1974; H. D. Megaw, *Acta Crystallogr.* **9,** 56 (1956).
17. R. D. Shannon, *Acta Crystallogr. Sect. B* **32,** 751 (1976).
18. W. L. Brown, R. E. Openshaw, P. F. McMillan, and C. M. B. Henderson, *Am. Mineral.* **69,** 1058 (1984).

19. J. V. Smith and W. L. Brown, ''Feldspar Minerals,'' Vol. 1, 2nd ed., p. 55. Springer, Berlin, 1988.
20. H. D. Megaw, ''The Feldspars'' (W. S. MacKenzie and J. Zussmann, Eds.), p. 87. University Press, Manchester, 1974.
21. J. V. Smith and W. L. Brown, ''Feldspar Minerals,'' Vol. 1, 2nd ed., p. 138. Springer, Berlin, 1988.
22. W. Joswig and W. H. Baur, *Neues Jahrb. Mineral. Monatsh.* 26 (1995).
23. W. H. Baur and R. X. Fischer, *Zeobase.* Frankfurt and Bremen (1995).
24. W. H. Baur, R. X. Fischer, and R. D. Shannon, ''Innovation in Zeolite Materials Science'' (P. J. Grobet, W. J. Mortier, E. F. Vansant, and G. Schultz-Ekloff, Eds.), p. 281. Elsevier, Amsterdam, 1988.
25. K. Snelson, ''The Nature of Structure.'' New York Academy of Sciences, New York, 1989.
26. G. M. Sheldrick, ''SHELXL-93. Program for refinement of crystal structures.'' Univ. Göttingen, Deutschland, 1993.
27. W. H. Baur and D. Kassner, *Z. Kristallogr. Suppl. Issue* **3,** 15 (1991).
28. A. F. Wells, *Acta Crystallogr.* **7,** 535 (1954).
29. A. F. Wells, ''Structural Inorganic Chemistry,'' 5th ed. Clarendon, Oxford, 1984.
30. A. F. Wells, ''Three-Dimensional Nets and Polyhedra.'' Wiley, New York, 1977.
31. A. F. Wells, ''Further Studies of Three-Dimensional Nets.'' American Crystallographic Association, Pittsburgh, 1979.
32. A. F. Wells, *Acta Crystallogr.* **7,** 545 (1954).